

An electromechanical impedance-based method for tensile force estimation and damage diagnosis of post-tensioning systems

Jiyoung Min^{1a}, Hyojin Shim², Chung-Bang Yun^{3b} and Jung-Wuk Hong^{*3}

¹Structural Engineering Research Institute, Korea Institute of Civil Engineering and Building Technology,
283 Goyangdae-ro, Ilsanseo-gu, Goyang-si, Gyeonggi-do 411-712, Korea

²Big Science Program Team, National Research Foundation of Korea,
201 Gajeong-ro, Yuseong-gu, Daejeon, 34113, Korea

³Department of Civil and Environmental Engineering, Korea Advanced Institute of Science and Technology,
291 Daehak-ro, Yuseong-gu, Daejeon 305-338, Korea

(Received February 28, 2015, Revised June 10, 2015, Accepted September 1, 2015)

Abstract. We propose an effective methodology using electromechanical impedance characteristics for estimating the remaining tensile force of tendons and simultaneously detecting damages of the anchorage blocks. Once one piezoelectric patch is attached on the anchor head and the other is bonded on the bearing plate, impedance responses are measured through these two patches under varying tensile force conditions. Then statistical indices are calculated from the impedances, and two types of relationship curves between the tensile force and the statistical index (TE Curve) and between statistical indices of two patches (SR Curve) are established. Those are considered as database for monitoring both the tendon and the anchorage system. If damage exists on the bearing plate, the statistical index of patch on the bearing plate would be out of bounds of the SR curve and damage can be detected. A change in the statistical index by damage is calibrated with the SR curve, and the tensile force can be estimated with the corrected index and the TE Curve. For validation of the developed methodology, experimental studies are performed on the scaled model of an anchorage system that is simplified only with 3 solid wedges, a 3-hole anchor head, and a bearing plate. Then, the methodology is applied to a real scale anchorage system that has 19 strands, wedges, an anchor head, a bearing plate, and a steel duct. It is observed that the proposed scheme gives quite accurate estimation of the remaining tensile forces. Therefore, this methodology has great potential for practical use to evaluate the remaining tensile forces and damage status in the post-tensioned structural members.

Keywords: piezoelectric patches; impedance; tensile force estimation; damage diagnosis

1. Introduction

Prestressing systems developed for many years represent a major advancement in construction technology. A predetermined compressive force is applied to concrete before loading, and this

*Corresponding author, Associate Professor, E-mail: j.hong@kaist.ac.kr

^a Research specialist

^b Emeritus Professor

force reduces the tensile stress in the section so that the tensile stress is below the cracking stress. Thus, many civil engineers have utilized prestressing techniques in long-span bridges, slabs in buildings, water tanks, concrete piles, thin shell structures, offshore platforms, and nuclear containment structures (Ashar *et al.* 1994, Beard1 *et al.* 2003, Hyunh *et al.* 2015, Rogowsky *et al.* 1991).

There are two types of prestressing systems, pre-tensioning and post-tensioning (Raju 2006). Post-tensioning system is a form of prestressed concrete in which the load resistance of the overall structure increases as the prestressing tendon is stressed after hardening of the concrete, whereas in the pre-tensioning system, the tendon is stressed prior to concrete placement. Unlike pre-tensioning, post-tensioning tendons are usually anchored using mechanical anchorage devices, which provide a clearly defined anchorage for the tendon (Rogowsky *et al.* 1991). The anchorage device commonly consists of wedges, an anchor head, a bearing plate, a sheath or duct, and grout connection (Schechter *et al.* 1970). Among these, the anchor head and the bearing plate are mainly responsible for transferring the prestress into the concrete, therefore any deterioration in carrying tensile force or damage of the anchorage needs to be carefully monitored.

The lift-off test is conventionally applied in the field to measure the tensile force of tendon. However, it is very time-consuming, expensive, and laborious. Furthermore, it is difficult to use during the normal operational period between regular inspections. To overcome these limitations, many investigations has been conducted for the tensile force estimation. A modal analysis-based approach has been employed for the measurement of stay cable force (Bati *et al.* 2001). A vibrometer has been utilized to measure low-level cable vibrations under ambient excitations. Researchers proposed a relationship between the natural frequency and the cable tension such that the stay cable force can be rapidly estimated by extracting natural frequencies from vibration responses. Kim *et al.* (2010) suggested a new method based on longitudinal waves. Longitudinal vibration was measured along the tendon, and then a relationship was derived in terms of the tensile force, the elastic wave velocity, and the elastic modulus. Through several experimental studies, they showed that the wave velocity increases nonlinearly as the tensile force level increases. Nguyen *et al.* (2012) and Huynh *et al.* (2015) proposed an electromechanical (E/M) impedance-based technique introducing an interface washer inserted into an anchorage block. A piezoelectric patch was attached on the washer, and the loss of tensile force was detected by monitoring the stress change or the change in impedance of the washer. Experimental studies were performed on a prestressed concrete girder, and this technique could be effectively applied when insufficient space exists to attach the piezoelectric patch to the structure directly or when impedance signatures are very weak and thus difficult to analyze.

Studies aimed at detecting damage to tendons and near anchorage zones have been carried out by several researchers. Sansalone *et al.* (1996) investigated using the impact echo method to detect voids in tendon ducts of post-tensioned concrete slab. A short duration mechanical impact generated low-frequency waves at a free surface, and the waves propagated through the thickness of the structure. When waves meet a void, several parts of the waves are reflected to the free surface and the void could be detected. A method utilizing magnetic flux leakage gained some interest, especially in Europe (Bouchilloux *et al.* 1999). This method is based on the fact that a flaw in a ferromagnetic object causes a localized discontinuity in the magnetic properties of the system.

In this paper, we propose a new and effective methodology for both estimating the tensile force of the tendon and detecting damage occurring at the vicinity of the anchorage using the impedance technique with multiple piezoelectric patches. First, impedance-based techniques are briefly

summarized, and the procedure of the proposed approach is described. Then, experimental studies are presented: The approach is validated in a 3-hole simplified anchorage system with artificial damage and is applied to a real scale 19-strand anchorage system under varying tensile force conditions.

2. Theoretical background

2.1 Electromechanical Impedance

For electromechanical (E/M) impedance-based techniques, small piezoelectric patches are popularly used. Those patches are attached on a target structure, and the responses are analyzed for the estimation of the structural integrity. The fundamental mechanism of this active sensing technology is energy transfer between the patch and the host mechanical system. If a piezoelectric ceramic (PZT) patch is excited with a high-frequency sinusoidal voltage, it causes the local area of the structure to vibrate (the converse piezoelectric effect) and the structural response is converted to the electrical response of the PZT by the direct piezoelectric effect. Thus, the mechanical impedance of the structure is directly correlated with the electrical impedance of the patch. The coupled E/M impedance $Z(\omega)$ is easily measured using an instrument such as an Agilent 4294A, and it is expressed analytically as

$$Z(\omega) = [j\omega C(1 - \kappa_{31}^2 \frac{Z_s(\omega)}{Z_a(\omega) + Z_s(\omega)})]^{-1} \quad (1)$$

where C is the zero-load capacitance of the PZT, κ_{31} is the E/M coupling coefficient of the PZT, Z_s is the impedance of the host structure, and Z_a is the impedance of the PZT (Liang *et al.* 1996). Given that the geometric and material properties of the PZT stay constant, Eq. (1) shows that a change in a structure's mechanical impedance directly results in a change of the E/M impedance measured by the PZT. Because damage causes changes in the local mass, stiffness, and/or damping properties and consequently its mechanical impedance, the mechanical integrity of the structure can be assessed by monitoring E/M impedance. It should be noted that the E/M impedance is a complex number. The real part of impedance (resistance) reacts more sensitively to structural damage than does the imaginary part (reactance). On the other hand, reactance is mostly used for the self-diagnosis of piezoelectric patches because PZTs are capacitive devices and their impedance value is dominated by the imaginary part of $j\omega C$ (Bhalla *et al.* 2002, Min *et al.* 2010, Park *et al.* 2006).

2.2 A Statistical index for impedance-based structural health monitoring

Assessments about the integrity of host structures are performed by analyzing certain changes in E/M impedance. Impedance changes provide only qualitative information on the status of the structure without any specific information such as damage severity or location. Thus, several statistical scalar indices are used to evaluate structural health quantitatively, and they have the merit of being easily calculated when only two signals are given. Among them, the root mean square deviation (RMSD) and the cross-correlation coefficient (CC) are commonly used for

impedance methods (Peairs *et al.* 2006). These metrics employ the difference between two impedance values at each frequency component.

$$\text{RMSD} = \sqrt{\frac{\sum_{i=1}^n \{\text{Re}(Z_0(\omega_i)) - \text{Re}(Z_0(\omega_i) - \delta)\}^2}{\sum_{i=1}^n \text{Re}(Z_0(\omega_i))^2}} \quad (2)$$

$$\text{CC} = \frac{1}{N} \sum_{i=1}^N \frac{\{\text{Re}(Z_0(\omega_i)) - \bar{Z}_0\} \{\text{Re}(Z_1(\omega_i)) - \bar{Z}_1\}}{\sigma_{Z_0} \sigma_{Z_1}} \quad (3)$$

where $Z_0(\omega)$ is the impedance of the PZT measured in the healthy condition (baseline); $Z_1(\omega)$ is the impedance in the current condition; n is the number of frequency points; \bar{Z}_0 and \bar{Z}_1 are mean values of $\text{Re}(Z_0(\omega))$ and $\text{Re}(Z_1(\omega))$; σ_{Z_0} and σ_{Z_1} are standard deviations of $\text{Re}(Z_0(\omega))$ and $\text{Re}(Z_1(\omega))$; and δ is the difference between \bar{Z}_0 and \bar{Z}_1 . These metrics are scaled by the baseline measurement, and vertical shifts are corrected by subtracting mean values from the interrogation impedance. Here, the vertical shift does not indicate a damage event but rather a change in environmental conditions such as temperature and humidity. With the RMSD metric, the amplitude variation of the impedance is mainly compared. The greater the value of the metric, the larger the difference between the baseline and the subsequent reading, which means a greater likelihood of damage in a structure. On the other hand, the CC metric compares the shape change of the impedance. The smaller the value of the CC metric, the larger the difference between those impedances and the likelihood of damage (Min *et al.* 2010).

3. Proposed scheme for monitoring tensile force and damages in anchorage system

This study focuses on the development of a simple and easily applicable monitoring methodology for anchorage zones employing multiple piezoelectric patches: piezoelectric patches attached on the anchor head estimate the tensile force of the tendon, and piezoelectric patches attached on the bearing plate or the concrete zone evaluate damage near the anchorage zone. This scheme is based on the idea that impedance signals are sensitive to localized structural changes if the sensing area is not large. This means that the piezoelectric patch on the anchor head has difficulty in detecting damage existing near the bearing plate or concrete zone, and vice versa.

Suppose that one piezoelectric patch (Patch A) is attached on an anchor head and the other (Patch B) on a bearing plate. The proposed method makes use of (1) the relationship between the tensile force and the statistical index of Patch A and/or Patch B for monitoring the tension loss, and (2) the relationship between the statistical indices of Patches A and B for diagnosing damage in the anchorage zone. In this study, the RMSD index is utilized to quantify the impedance variation considering that peak frequencies primarily change under external loads, and this can be more easily detected using the RMSD index than the CC index (Min *et al.* 2012).

First, impedance signals are measured through Patches A and B depending upon tensile forces. The RMSD value is calculated from each impedance reading, and then two TE curves are

constructed describing the relationship between the tensile force and the RSMD index of each sensor. An SR curve is also formulated from the relationship between the RMSD indices of Patches A and B for damage diagnosis. These three curves (two TE curves and one SR curve) are stored as baseline data, which can be obtained during the early stage of construction or during regular inspection of a structure. After the baseline is established, impedance signals are continuously measured through Patches A and B. RMSD values are calculated and first compared with the SR curve. If they stay inside the pre-determined threshold, the structure is diagnosed as healthy. Otherwise, it is considered to be damaged, and the RMSD values are corrected by the SR curve. Description of the correction method is given later at Section 4.3. The tensile force is finally estimated with the calculated or corrected RSMD value using the TE curve of each sensor. The procedure of the proposed method is described in Fig. 1.

4. Experimental validation on a simplified anchorage system

To validate the proposed method, experimental studies were performed on a 3-strand anchorage system. Impedance signatures were measured through two piezoelectric patches attached onto the anchor head and the bearing plate. RMSD values were calculated under varying applied tensile force conditions and two TE curves for tension estimation and a SR curve for damage diagnosis were constructed as a database. Then the bearing plate was artificially damaged and investigated with the SR curve to correct RMSD values. With the pre-constructed TE curves, the unknown tensile force as well as the damage status of the anchorage system were finally estimated.

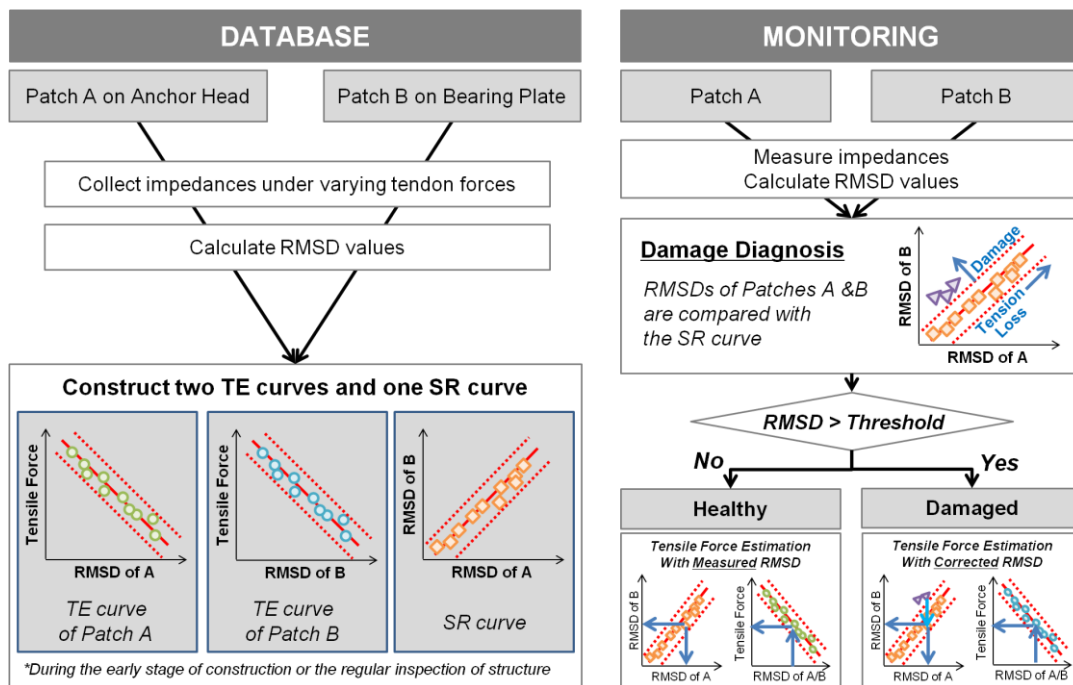


Fig. 1 Scheme of the proposed method

4.1 Experimental setup

The target specimen was a 3-strand anchorage system consisting of three solid wedges, a 3-hole anchor head (the diameter of 90 mm), and a bearing plate (the diameter of 180 mm). The tensile force on the tendon, actually applied on the anchorage block, was simplified to an external compressive load through three solid wedges. This simplified system reduced the cost of the experimental setup in order to apply effective tensile force to the tendon and the anchorage system because it does not require actual strands, a concrete beam, and a hydraulic jacking device.

An MFC patch (MFC #1) was attached to the side of the anchor head and a PZT patch (PZT #1) to the top of the bearing plate (Fig. 2). The dimensions of MFC #1 are 85x28x0.3 mm, and those of PZT #1 are 25x25x0.2 mm. MFC patches are very flexible, so it is possible to bond them onto a curved surface, but their performance is markedly lower compared to that of a PZT patch. These two patches were connected to a conventional impedance measuring device (Agilent 4294A) through a multiplexer (Agilent 34980A with 34921A). The specimen was placed in the UTM equipment as shown in Fig. 3, and then an initial compressive load of 20 tonf was applied onto three solid wedges that precisely control the eccentric force. In total, 11 load cases were tested with a gradual decrease of the force by 2 tonf. These 11 steps were repeated three times to confirm the reproducibility of the proposed method.

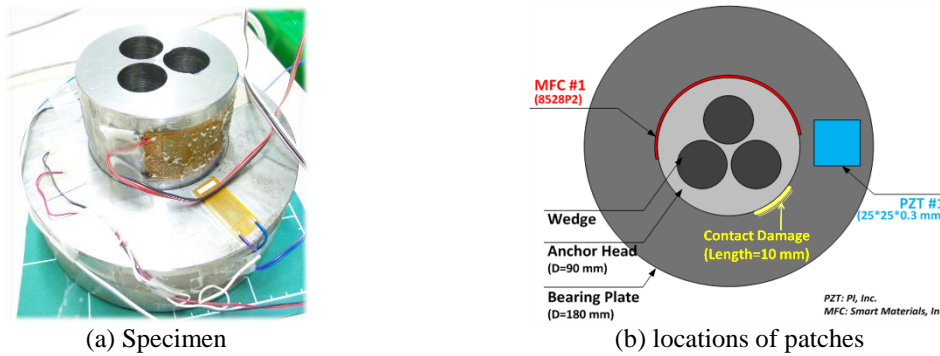


Fig. 2 Three-strand anchorage system

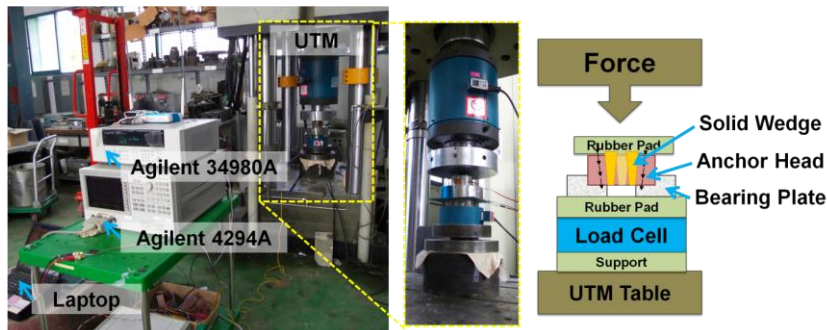


Fig. 3 Experimental setup for validation tests

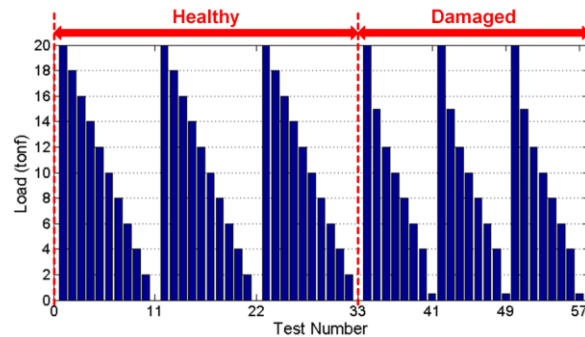


Fig. 4 Loading scenario

For damage diagnosis, damage was simulated on the surface of the bearing plate engaged with the anchor head, simulating excessive stress highly concentrated on a certain point due to an uneven tensile force of the tendon. As described in Fig. 2(b), the dimensions of damage are 10 mm in length and 1 mm in depth. Then, a compressive load of 20 tonf was initially applied and gradually decreased. The test was repeated three times according to the loading scenarios described in Fig. 4. It should be noted that the room temperature remained constant at approximately 23°C during all experiments to remove the effect by temperature on the impedance signal.

4.2 Impedance signatures and statistical indices

Impedance signals were measured at each load case in the frequency range of 110 to 160 kHz for MFC #1 and 25 to 45 kHz for PZT #1. The frequency ranges were selected considering resonant peaks related to the dynamic interaction between the piezoelectric patch and the structure. The measured signals and variations were presented in Fig. 5. In both the MFC #1 and PZT #1 patches, the anti-resonance peaks shifted leftwards, and their magnitudes varied as the load decreased. The strain/stress from the induced compressive load might change the system properties of the combined structure such as natural frequencies, and consequently shift its anti-resonance peak (Giurgiutiu 2008, Min 2012) because anti-resonance peaks are substantially influenced by the natural frequency of the structure.

Damage was artificially induced on the surface of the bearing plate near PZT #1 to consider both tensile force and damage effects. All signals measured under varying loading conditions and several representative samples showing signal variation due to damage are shown in Fig. 6. MFC #1, located far from damage, was not greatly affected by damage, whereas signals from PZT #1 varied considerably. Thus, the presence of damage and its approximate location could be estimated by comparing the responses of the two patches.

The RMSD index defined in Eq. (2) was then calculated to quantify resistance variations, as shown in Fig. 7. In the healthy condition, the RMSD values of MFC #1 and PZT #1 increased by approximately 0.025 and 0.08, respectively, with a 2 tonf load decrease. When damage was induced, the RMSD values of PZT #1 increased markedly relative to the healthy condition, while those of MFC #1 remained within bounds. Thus, damage occurring near the patch can be detected through impedance variation, and it can be localized by using an array of piezoelectric patches.

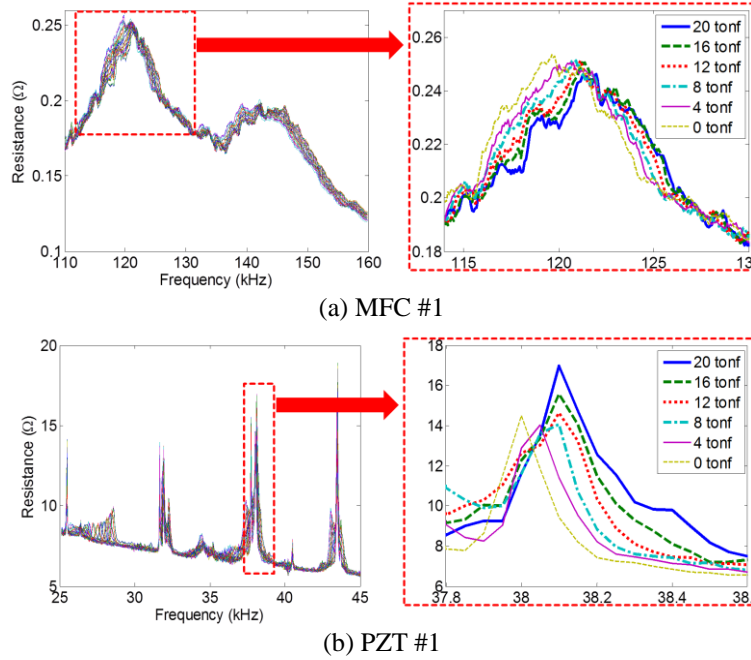


Fig. 5 Variation of tensile-force dependent resistance

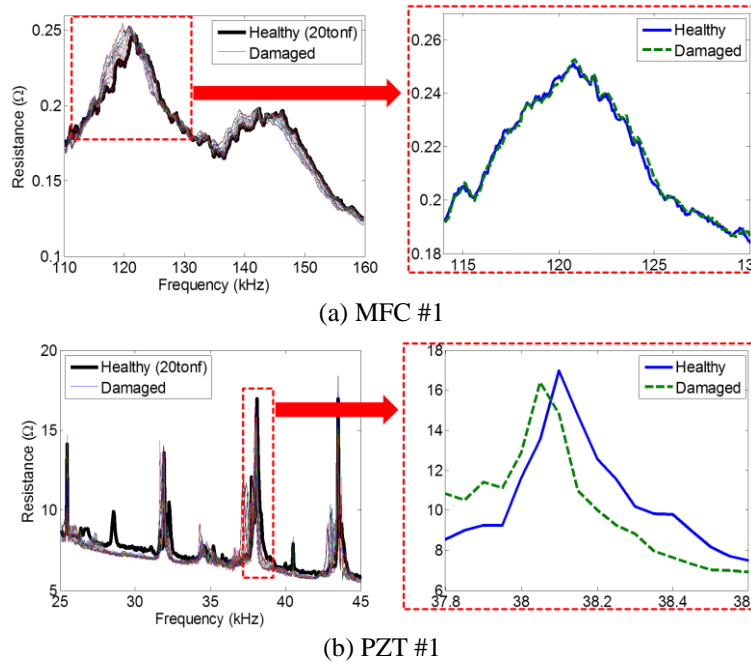


Fig. 6 Variation of damage dependent resistance

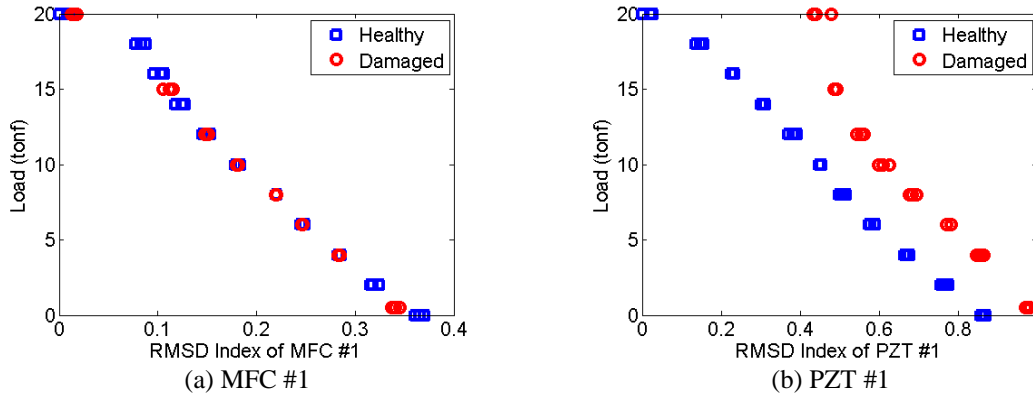


Fig. 7 Variation of RMSD for loads

4.3 Tensile force estimation and damage diagnosis

The relationship between the RMSD index and the load in the intact condition was formulated through linear regression analysis in order to estimate unknown tensile forces from RMSD values. Data from the first loading cycle were used to set the regression curve (which could be acquired in the field during construction or regular inspections), and it was evaluated with data from the second two loading cycles.

The results of the regression analysis for the intact case from the data of MFC #1 and PZT #1 are displayed in Fig. 8. The filled squares represent the baseline, the triangles indicate the validation of the analysis, the circles indicate the damaged condition, the solid line is the TE curve, and the two dotted lines are the 99% confidence level (C.L.) of the TE curve. The baseline data from the two patches are used to make TE curves with RMS errors of 0.737 and 0.585, respectively. When damage occurred near PZT #1 and far from MFC #1, the RMSD values of PZT #1 exceeded the 99% C.L., while those of MFC #1 remained within bounds.

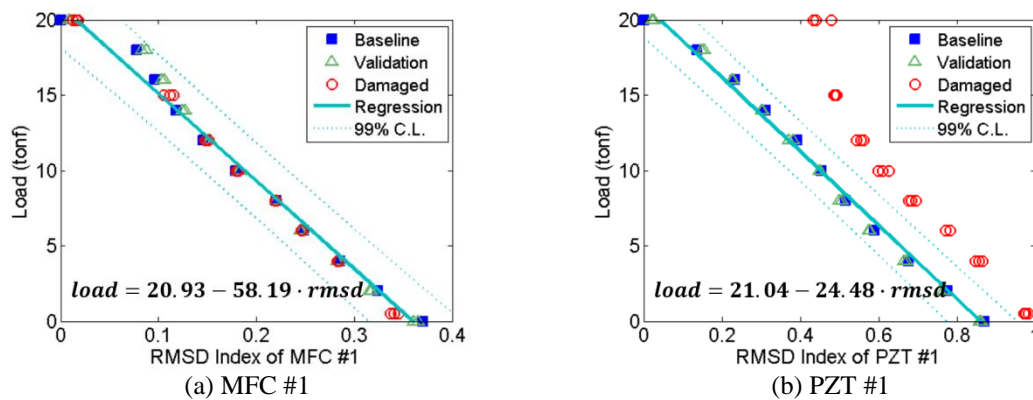


Fig. 8 TE curves for the estimation of tensile force

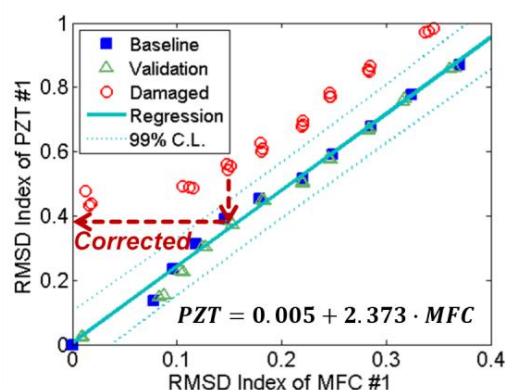


Fig. 9 SR curve for damage evaluation

Increased RMSD due to damage might lead to a false alarm that the tensile force has decreased when it has remained constant. To avoid this problem, SR curves from patches placed at different locations under the intact condition can be calculated. SR curves are able to provide information about the quantity and location of damage. Although the curve between the RMSD a linear regression analysis was performed to approximate the relationship. Fig. 9 shows an SR curve and its 99% C.L., where the RMS error was 0.025, which is small enough to evaluate damage. It was found that data from PZT #1 in the damaged case were out of the C.L., whereas those of MFC #1 remained within bounds. Thus, damage could be diagnosed using this SR curve by checking whether the RMSD value is within bounds. If the RMSD value is out of bounds, it should be corrected to estimate the tensile force, as described with a dotted arrow in Fig. 9. For example, when the RMSD value of PZT #1 is 0.6 and that of MFC #1 is 0.15, the RMSD value of PZT #1 is corrected to 0.36 with the SR curve, and then the tensile force is estimated using the TE curves.

Two TE curves and one SR curve were constructed as baseline data for both tensile force estimation and damage diagnosis. Samples of estimated tensile force are shown in Fig. 10, wherein RMSD values from the second loading cycle in the intact condition were used together with values from the second loading cycle in the damaged condition. The estimated forces showed good agreement with the forces actually applied. In the case of MFC #1, maximum errors of 1.92 tonf (healthy) and 0.60 tonf (damaged) occurred between the actual value and estimated values, while errors of 0.88 tonf (healthy) and 0.60 tonf (damaged) were observed when the RMSD values of PZT #1 were used. For the damaged case the corrected RMSD values of PZT#1 were used. These results indicate that the proposed method can provide reasonable estimations of the remaining tensile force and the damage status of the anchorage structure using only RMSD values calculated from the impedances of multiple patches.

However, in order to improve the sensitivity of this approach, the appropriate selection of measuring frequency and the noise reduction including ambient and instrumental effects are still very important although this method uses high frequency band and environmental noise is lower than a few kHz. Especially, the optimal measuring frequency needs to be determined considering the geometric and material properties of a piezoelectric patch and a target structure. The accurate decision might be achievable through further in-depth studies in the impedance-based technology.

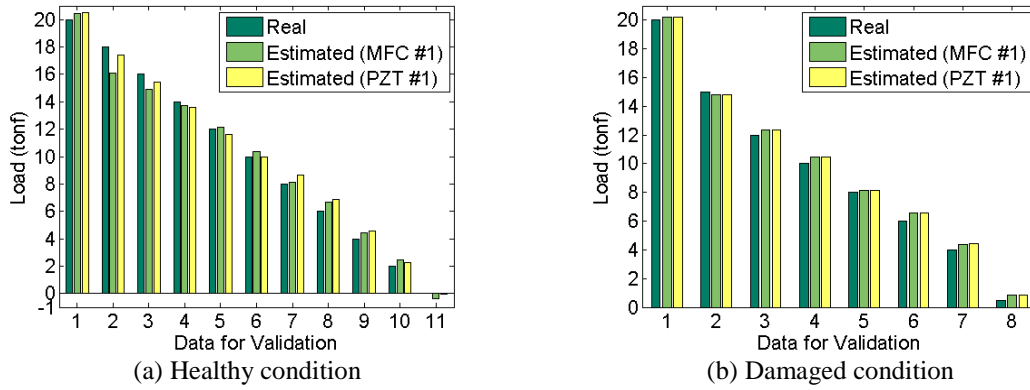


Fig. 10 Estimated tensile forces using the proposed method

5. Application on a real-scale anchorage system

The proposed methodology is applied on a real-scale anchorage system that consists of 19 strands. These strands are usually used for post-tensioning of concrete bridges. By changing loads on the strands, impedance signatures were measured from four piezoelectric patches that are attached on the anchor head and the bearing plate. RMSD values were calculated and TE curves and SR curves were constructed to estimate the remaining tensile force and damage. With the pre-constructed TE curves, the unknown tensile force as well as the damage status were calculated through blind tests.

5.1 Experimental setup

A 19-strand anchorage system was set up as a target structure for the application of the proposed approach. The system consists of 19 strands (the diameter of 15.2 mm), wedges, an anchor head (the diameter of 230 mm and the height of 95 mm), a square bearing plate (the size of 340x340x50 mm), and a steel duct (the diameter of 116 mm and the thickness of 3 mm). A steel body frame was stressed through this system as displayed in Fig. 11.

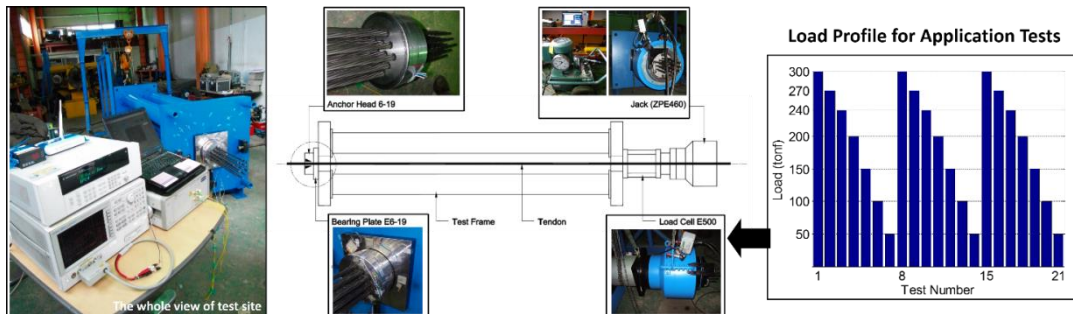


Fig. 11 Overview of application tests

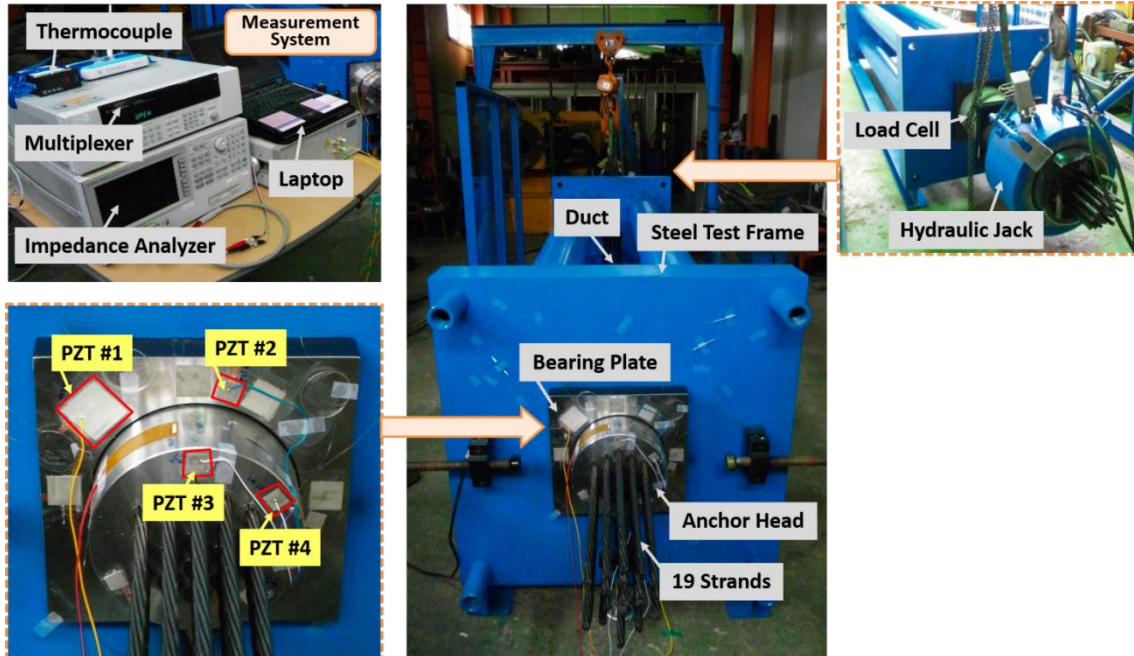


Fig. 12 Experimental setup for real application on 19-strand anchorage system

Two PZT patches, PZT #1 of 50x50x0.3 mm and PZT #2 of 20x20x0.3 mm, were surface-mounted on the top of the bearing plate. Other two PZT patches of 20x20x0.3 mm were attached on the top of the anchor head. The specific experimental setup including information on patch locations is illustrated in Figure 12. Four PZT patches were connected to a conventional impedance measuring device (Agilent 4294A) through a multiplexer (Agilent 34980A with 34921A). Frequency ranges for impedance measurements were selected as 45-75 kHz for PZT #1, 65-85 kHz for PZT #2, 74-85 kHz for PZT #3, and 90-110 kHz for PZT #4, which were selected considering resonant peaks related to the dynamic interaction between the piezoelectric patch and the structure. The room temperature was controlled constant about 10°C and monitored through a thermocouple (Asahi Keiki A5113-13).

19 strands were tensioned by a hydraulic jacking device (VSL Korea, ZPE460) and compressive stress was applied into the overall system. A maximum tensile force of 300 tonf was applied first, which was determined by considering the number of strands and the ultimate tensile force of each, and then gradually decreased upto 50 tonf in 7 steps: 300 tonf, 270 tonf, 240 tonf, 200 tonf, 150 tonf, 100 tonf, and 50 tonf. This procedure was repeated three times to construct the baseline of this system.

5.2 Tensile force estimation

Impedance signals were measured for each loading case in the pre-decided frequency range from each PZT patch. As explained in Section 4.2, most of signals including several anti-resonance peaks shifted leftward as the tensile force reduced with the variation of the structural local resonant property. RMSD indices were calculated from the baseline obtained with the initial loading of 300

tonf. All RMSD values linearly decreased with the reduction of tensile force, which should be investigated mechanically and numerically further. The RMSD values of PZT #1~#4 increased by approximately 0.15, 0.13, 0.25, and 0.13, respectively, with a 50 tonf load reduction.

The relationship between the RMSD index and the load in the intact condition was formulated through linear regression analysis. All the process was same with Section 4 and the results of the regression analysis were displayed in Fig. 13. The filled squares represent the baseline of the first two cycle loadings, the triangles indicate the validation data of regression in the third cycle loading, the solid line is the TE curve, and the two dotted lines are the 99% C.L. of the TE curve. The RMS errors of regression were 4.87, 4.87, 9.96, and 11.08, respectively. Fig. 14 showed one example of SR curve obtained from PZT #1 on the bearing plate and PZT #3 on the anchor head for baseline.

After regression curve of each patch was constructed with known loading cases, blind tests were finally carried out to guess the tensile force applied on the anchorage system. Impedance signals were first recorded through the prepared measuring equipment, RMSD values were calculated from resistance signals, and tensile forces were estimated based on pre-constructed TE curves.

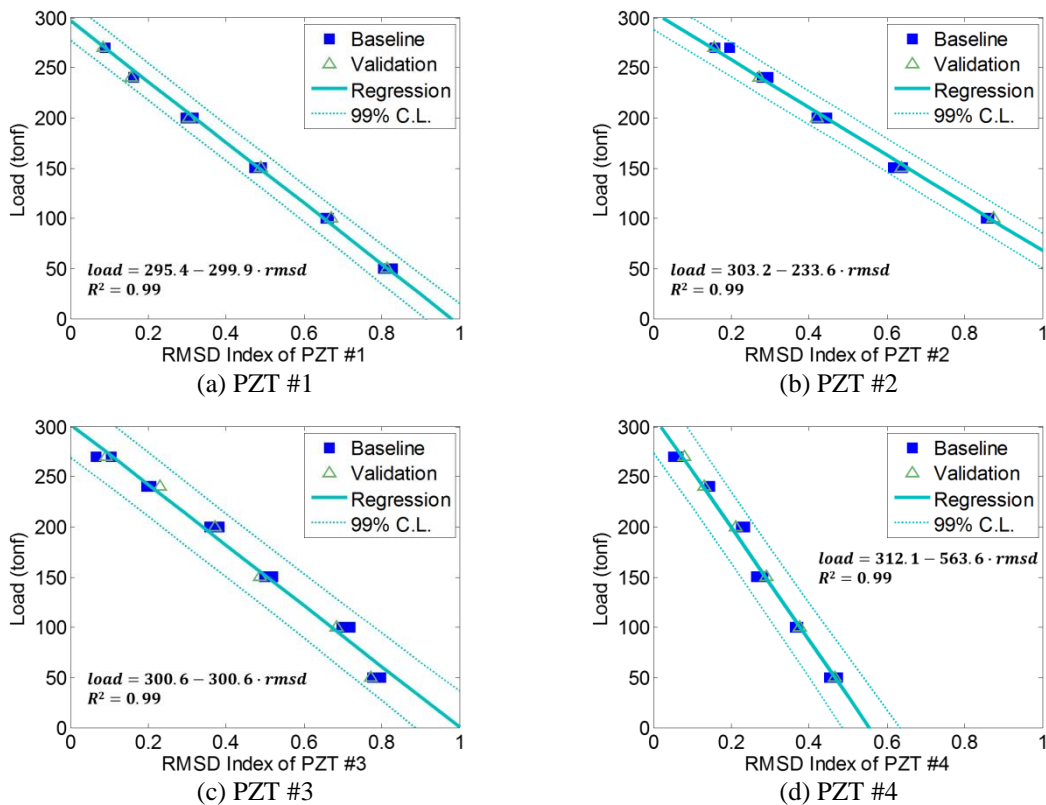


Fig. 13 TE curves of four PZT patches on 19-strand anchorage system

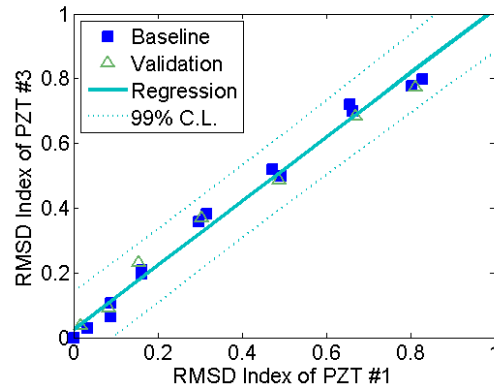


Fig. 14 SR curve between PZT #1 and PZT #3

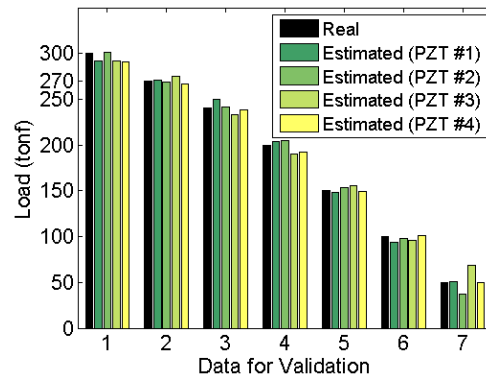


Fig. 15 Estimated tensile forces on 19-strand anchorage system

Fig. 15 shows the final results of estimations from four PZT patches, compared to the real force values actually applied to the target system. They are in good agreement and the maximum errors of 19 tonf occurred at 250 tonf reduction of tensile force. The proposed method needs pre-constructed baseline such as TE curves, but these can be easily obtained during construction or a regular inspection. The results of blind tests indicated that the proposed method has big potential to evaluate the tensile force applied through strands on the anchorage system and mutuality between patches at different spots can also provide the information on damage status.

6. Conclusions

In this paper, we proposed an effective structural health monitoring methodology to simultaneously estimate the tensile force of the prestressed tendon and monitor the structural integrity of the anchorage zone using an impedance-based method. A TE curve was constructed for

each patch based on the relationship between the RMSD index and the tensile force, and an SR curve was formulated based on the relationship between the RMSD indices of two patches attached at different locations, i.e., on the anchor head and the bearing plate. These curves and a pre-constructed threshold were saved as baseline. Then impedance responses were monitored, and RMSD index values were calculated periodically. These patch RMSD values were first compared to the SR curve for damage diagnosis. If the value was within bounds, the structure could be determined to be undamaged. On the other hand, if the value was out of bounds, the structure could be considered to be damaged, and RMSD values needed to be corrected using the SR curve. The calculated or corrected RMSD value of each patch was used as an input into the TE curve, and then the tensile force could be calculated. The proposed approach was validated successfully through two experimental studies on a simplified 3-hole anchorage system and on a real scale 19-strand anchorage system. The results showed its great potential for practical use for the purpose of both tensile force estimation and damage diagnosis in post-tensioned members.

Acknowledgements

This work was financially supported by the Innovations in Nuclear Power Technology of the Korea Institute of Energy Technology Evaluation and Planning (KETEP) grant funded by the Korea government Ministry of Knowledge Economy (No. 20101620100090), and was supported by the 2012 research fund (1.120007) of Ulsan National Institute of Science and Technology (UNIST). Authors also thank VSL Korea for the support of the real scale experiments.

References

- Al-Omaishi, N., Tadros, M.K. and Seguirant, S.J. (2009), "Estimating prestress loss in pretensioned, high-strength concrete members", *PCI J.*, **54**(4), 132-159.
- Ashar, H., Naus, D. and Tan, C.P. (1994), "Prestressed Concrete in U. S. Nuclear Power Plants (Part 1)", *Concrete Int.*, **16**(5), 30-34.
- Bati, S.B. and Toniatti, U. (2001), "Experimental methods for estimating in situ tensile force in tie-rods", *J. Eng. Mech. - ASCE*, **127**(12), 1275-1283.
- Beard1, M.D., Lowe, M.J.S. and Cawley, P. (2003), "Ultrasonic Guided Waves for Inspection of Grouted Tendons and Bolts", *J. Mater. Civil Eng. - ASCE*, **15**(3), 212-218.
- Bhalla, S., Naidu, A.S.K. and Soh, C.K. (2002), "Influence of structure-actuator interactions and temperature on piezoelectric mechatronic signatures for NDE", *Proceedings of the ISSS-SPIE Int'l Conferences on Smart Materials Structures and Systems*, Bangalore, December.
- Giurgiutiu, V. (2008), *Structural health monitoring with piezoelectric wafer active sensors*, Elsevier/Academic Press, Amsterdam.
- Hyunh, T.C., Lee, K.S. and Kim, J.T. (2015), "Local dynamic characteristics of PZT impedance interface on tendon anchorage under prestress force variation", *Smart Struct. Syst.*, **15**(2), 375-393.
- Kim, B.H., Jang, J.B., Lee, H.P. and Lee, D.H. (2010), "Effect of prestress force on longitudinal vibration of bonded tendons embedded in a nuclear containment", *Nuclear Eng. Des.*, **240**(6), 1281-1289.
- Koo, K.Y., Park, S., Lee, J.J. and Yun, C.B. (2009), "Automated impedance-based structural health monitoring incorporating effective frequency shift for compensating temperature effects", *J. Intel. Mat. Syst. Str.*, **20**, 367-377.
- Liang, C., Sun, F.P. and Rogers, C.A. (1996), "Electro-mechanical impedance modeling of active material systems", *Smart Mater. Struct.*, **5**(2), 171-186.

- Min, J. (2012), *Structural Health Monitoring for Civil Infrastructure Using Wireless Impedance Sensor Nodes and Smart Assessment Techniques*, KAIST, Doctoral Dissertation.
- Min, J., Park, S., Song, B.H. and Yun, C.B. (2010), "Development of wireless sensor nodes for impedance-based structural health monitoring", *Smart Struct. Syst.*, **6**, 689-709.
- Nguyen, K.D. and Kim, J.T. (2012), "Smart PZT-interface for wireless impedance-based prestress-loss monitoring in tendon-anchorage connection", *Smart Struct. Syst.*, **9**(6), 489-504.
- Park, G., Farrar, C.R., Rutherford, A.C. and Robertson, A.N. (2006), "Piezoelectric active sensor self-diagnostics using electrical admittance measurements", *J. Vib. Acoust.*, **128**(4), 469-476
- Park, G., Sohn H., Farrar, C.R. and Inman, D.J. (2003), "Overview of piezoelectric impedance-based health monitoring and path forward", *Shock Vib. Digest*, **35**(6), 451-463.
- Peairs, D.M., Tarazaga, P.A. and Inman, D.J. (2006), "A study of the correlation between PZT and MFC resonance peaks and damage detection frequency intervals using the impedance method", *Proceedings of the International Conference on Noise and Vibration Engineering*, Leuven, Belgium, September.
- Raju, K. (2006), *Prestressed Concrete*, Tata McGraw-Hill Education, India.
- Rogowsky, D.M. and Marti, P. (1991), *Detailing for post-tensioned*, VSL International Ltd, Bern, Switzerland.
- Sansalone, M., Jaeger, B.J. and Randall, W.P. (1996), "Detecting voids in grouted tendons of post-tensioned concrete structures using impact-echo method", *ACI Struct. J.*, **93**(4), 462-472.
- Schechter, E. and Boecker, H.C. (1970), "Wedge anchorage system for strand post-tensioning", *Proceedings of the 6th Congress of the Federation Internationale de la Precontrainte*, Prague, Czechoslovakia, June.